

$U^{238}(n,2n)U^{237}$ Cross Section from 6 to 10 Mev*

J. D. KNIGHT, R. K. SMITH, AND B. WARREN

Los Alamos Scientific Laboratory, University of California, Los Alamos, New Mexico

(Received June 4, 1958)

The cross section for the $U^{238}(n,2n)U^{237}$ reaction has been measured with incident neutron energies from 6 to 10 Mev and at 16 Mev. The $(n,2n)$ cross section at each neutron energy was obtained by multiplying the ratio of U^{237} atoms to fission events, measured radiochemically, by the appropriate U^{238} fission cross section. These data, together with the data of other investigators for the 13–15 Mev region, are used to outline an $(n,2n)$ cross-section curve from threshold to 16 Mev.

INTRODUCTION

IN the past few years a number of measurements have been made of the cross sections for the nonelastic reactions of intermediate-energy neutrons with U^{238} . The total nonelastic cross section has been measured over the energy range 0.15–7.0 Mev^{1–3} and at 14 Mev.^{4,5} The neutron radiative capture cross section has been measured at energies up to 4 Mev,⁵ and the fission cross section at energies up to 21 Mev.^{6,7}

From these data, it is possible to account for the contributions of the various types of nonelastic reactions at neutron energies up to about 6 Mev. Above this region, the $(n,2n)$ reaction begins to constitute a significant part of the nonelastic events. To date, it has not been possible to determine the $(n,2n)$ events satisfactorily by purely physical techniques. The neutrons emitted are obscured by those from fission and the scattering process, and the end-product, U^{237} , is difficult to detect in the presence of the radiations from the fission products and UX_1 – UX_2 also present in the target material.

The present work consists of a measurement of the $U^{238}(n,2n)U^{237}$ cross section over the neutron energy range from threshold to 10 Mev and at 16 Mev by radiochemical isolation and absolute beta counting of the U^{237} produced. The procedure employed was essentially the following: small samples of U^{238} were exposed to neutrons from the $D(d,n)He^3$ reaction [or in the case of the 16-Mev irradiation, from the $T(d,n)He^4$ reaction] and analyzed radiochemically for fission-product Mo^{99} and for U^{237} . The Mo^{99} production per fission was determined in separate experiments at representative neutron energies by measuring directly the number of fissions

in thin U^{238} foils exposed back-to-back with thick samples which were subsequently analyzed for this fission product. The $(n,2n)$ cross sections were then obtained by multiplying the observed $(n,2n)$ /fission ratios by the fission cross sections previously measured at this Laboratory.⁷

EXPERIMENTAL METHODS

Neutron Sources and Irradiations

The neutrons were produced by deuteron bombardment of deuterium or tritium gas at the large electrostatic accelerator at Los Alamos. The gas target⁸ and uranium sample arrangement are shown in Fig. 1. The deuterium gas targets were 9 mm in diameter and either 10 mm or 30 mm long, and were filled to absolute pressures of 160–300 cm Hg. The tritium gas target was 10 mm long and was filled to 257 cm pressure. The bombarding deuteron beam, magnetically analyzed and collimated to 0.1-inch diameter, entered the target gas through a pair of hydrogen-cooled end windows made of 0.1-mil nickel or 0.3-mil molybdenum.

The uranium samples consisted of metal with a U^{238}/U^{235} atom ratio approximately 3000/1, fabricated in the form of disks 0.125 inch in diameter and 0.040 inch thick. For each run, two of the disks were stacked together with their axis that of the deuteron beam and with their mid-plane 12 mm from the end of the gas target. In order that the required neutron fluxes might be obtained without excessive energy spread, the

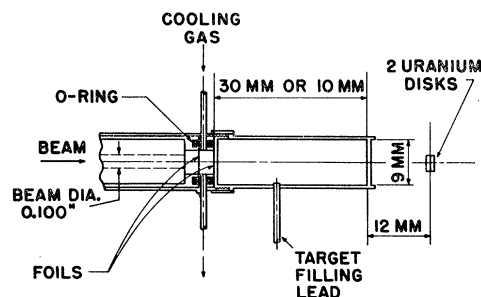


FIG. 1. Gas target and uranium sample arrangement.

* Work performed under the auspices of the U. S. Atomic Energy Commission.

¹ R. Batchelor, Proc. Phys. Soc. (London) A69, 214 (1956).

² Allen, Walton, Perkins, Olson, and Taschek, Phys. Rev. 104, 731 (1956), and Los Alamos Report LA-2099, April 29, 1957 (unpublished).

³ Beyster, Walt, and Salmi, Phys. Rev. 104, 1319 (1956).

⁴ Los Alamos unpublished work, cited by Coon, Davis, Felthaus, and Nicodemus, Phys. Rev. 111, 250 (1958).

⁵ Published and unpublished work in this field has been summarized by R. C. Allen and R. L. Henkel, in *Progress in Nuclear Energy, Physics and Mathematics Series I* (Pergamon Press, London, 1958), Vol. II.

⁶ R. W. Lamphere, Phys. Rev. 104, 1654 (1956).

⁷ Smith, Henkel, and Nobles, Bull. Am. Phys. Soc. Ser. II, 2, 196 (1957), and private communication.

⁸ The gas targets, intended for high-current use, were designed and built by R. A. Nobles, and are described in Rev. Sci. Instr. 28, 962 (1957).

uranium samples were exposed only at the position described, and a separate run was carried out for each neutron energy. The deuteron beam current at the target was adjusted to 4–8 microamperes, at which rate about 2–4 hours of machine time were required per run.

Radiochemical Analysis and Calibration

The irradiated uranium disks were dissolved separately and analyzed for U^{237} and Mo^{99} . The aliquots taken for uranium analysis were of a size such that the final purified sample contained 4–8 mg of uranium; the purified uranium was mounted as U_3O_8 on platinum plates and beta counted.

Inasmuch as the uranium was free of the U^{238} decay products UX_1 and UX_2 at the conclusion of the chemical analysis, the U^{237} counts had to be corrected for these beta-emitters as they grew back in. In practice, the U^{237} numbers were usually based on counting data taken during the first two days after preparation of the sample. UX counts were taken several months later, after disappearance of the U^{237} ; these latter counts gave a more reliable measure of the quantities of uranium than were obtained by weighing, and were used to determine the effective weights of the counting samples.

The calibration of the U^{237} beta counts in terms of atoms was established by two different methods. The first involved a comparison of counting rate under the adopted standard conditions with counting rate at 4π geometry; the second was derived by allowing a large sample of U^{237} to decay to Np^{237} and alpha counting the Np^{237} at known geometry. The U^{237} and Np^{237} half-lives were taken as 6.75 days and 2.20×10^6 years, respectively.

The calibration of Mo^{99} beta counts in terms of number of U^{238} fissions was conducted at 7.0- and 9.0-Mev neutron energies with the aid of a comparison fission counter. The uranium for radiochemical analysis consisted of a disk 1 inch in diameter and 0.040 inch thick, placed back-to-back with a second disk from which the fissions were measured directly; the second "disk" consisted of 2.955 g of U^{238} deposited as U_3O_8 over a 1-inch diameter circular area on a platinum foil. The fission counter was positioned so that the foils were normal to the axis of the deuteron beam and at a distance of 6 inches from the end of the gas target.

The final calibration factor, fissions per count/min Mo^{99} , was taken to be a linear function of neutron energy over the range 6–10 Mev; it varied from 2.26×10^5 at 6.0 Mev to 2.34×10^5 at 10.0 Mev.

The calibration factor at 14.1 Mev had been obtained earlier at this Laboratory by comparison fission counter measurements similar in principle though different in experimental detail. From this third calibration factor, which had a value of 2.56×10^5 , it was evident that the assumed linear relationship is no longer a good approxi-

mation in the 14-Mev range. The factor employed for the 16-Mev point, 2.69×10^5 , was estimated by extrapolation; relative to the others, it is probably accurate to $\pm 3\%$.

Of the two different types of calibration described above, that for U^{237} is considered to be the less accurate. The combination of U^{237} and Mo^{99} calibrations which enters into the ratio $(n,2n)/\text{fission}$ is estimated to be uncertain to $\pm 10\%$.

Measurements

From the separate analyses and beta counts performed on the two uranium disks irradiated in each run, two $(n,2n)/\text{fission}$ ratios were obtained. Although the more distant disk was shadowed slightly by the one in front, the $(n,2n)$ and fission numbers were assumed to be equally affected; accordingly, the $(n,2n)/\text{fission}$ ratios of front and rear disks were averaged.

The neutron energy is a direct function of deuteron energy and the angle between the incident deuteron and the emitted neutron traversing the disks. The deuteron beam had an energy spread due to straggling in the entrance foils and to degradation in the target gas; the latter was somewhat variable because of beam current effects. The angular spread of the neutrons traversing the disks was determined by the finite dimensions of both the disks and the deuteron beam, as well as by the initial angular spread of the deuterons due to Coulomb scattering in the target entrance foils.

Although an exact calculation of the effective neutron spectra at the disks is rather involved, graphical approximations have shown that the distributions in energy are approximately trapezoidal, with a skew toward the high-energy side. The neutron energy spectrum characteristic of each run was estimated graphically in terms of three quantities: an average energy, an exact upper energy, and effective lower energy. At the higher neutron energies with deuterium targets, it was necessary to take into account another effect: the production of additional fissions by a low-energy neutron component from the $D(d,np)D$ reaction. This effect was canceled out in the computations by the use of the "apparent" fission cross sections of Smith *et al.*,⁷ i.e., the preliminary cross sections before correction for the low-energy neutrons.

RESULTS

The experimental data and the cross sections derived from them are summarized in Table I. The neutron energy spreads shown are those defined by the upper and lower limits described in the previous paragraph. The error limits assigned to the $(n,2n)/\text{fission}$ and $(n,2n)$ cross-section values are relative, and refer to the analytical and counting data for each run; they are presented in this form to provide an indication of the

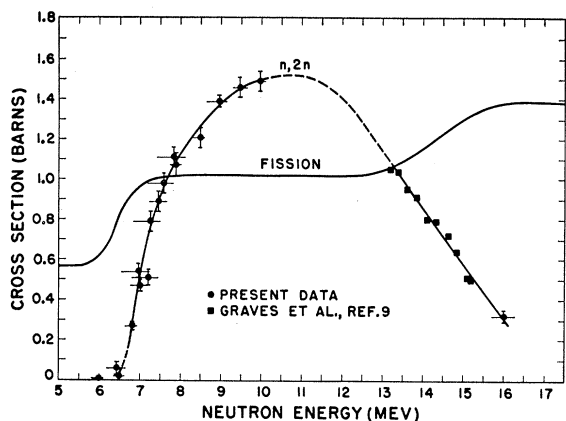


FIG. 2. U²³⁸(n,2n)U²³⁷ cross section versus neutron energy. Bracketed vertical lines represent uncertainties in individual analyses; over-all uncertainty in (n,2n) cross-section calibration is 15%. Horizontal lines represent total effective neutron energy spreads. Fission curve was obtained by smoothing out data of Smith *et al.*⁷

amount of error in individual determinations, as distinguished from the absolute error in the fission cross sections and the (n,2n)/fission ratio calibration. Thus, the over-all uncertainties in the (n,2n)/fission ratios are represented by the sum of the errors shown and the 10% uncertainty in the U²³⁷/Mo⁹⁹ calibration.

The uncertainties in the fission cross-section values are stated to be about 5%, of which about 3% is in the neutron flux determinations.⁷ Since the Mo⁹⁹/fission calibrations were performed with the same U²³⁸ foil with which the fission cross-section measurements were made, a small part of the error in the latter has already been taken into account. However, in view of the fact that the redundant portion is small, the over-all uncertainty in the (n,2n) cross sections will be considered to be 15% plus the data uncertainties listed in Table I.

The final (n,2n) cross-section data, together with the smoothed-out fission cross-section curve from

TABLE I. Summary of U²³⁸(n,2n)/fission and (n,2n) cross-section data.

Neutron energy (MeV) average spread	(n,2n)/fission ratio ^b	Apparent fission cross section ^a (barns)	(n,2n) cross section (barns)
5.98 _{-0.18} ^{+0.12}	(-0.02) ± 0.03	0.63	<0.01
6.42 _{-0.25} ^{+0.23}	0.08 ± 0.04	0.79	0.06 ± 0.03
6.49 _{-0.17} ^{+0.11}	<0.018	0.83	<0.02
6.80 _{-0.16} ^{+0.11}	0.30 ± 0.02	0.92	0.27 ± 0.02
6.96 _{-0.42} ^{+0.27}	0.56 ± 0.04	0.96	0.54 ± 0.04
7.00 _{-0.24} ^{+0.22}	0.48 _s ± 0.03	0.97	0.47 ± 0.03
7.20 _{-0.41} ^{+0.25}	0.51 ± 0.04	1.00	0.51 ± 0.04
7.25 _{-0.41} ^{+0.25}	0.79 ± 0.05	1.00	0.79 ± 0.05
7.45 _{-0.23} ^{+0.20}	0.88 ± 0.05	1.01	0.89 ± 0.05
7.58 _{-0.40} ^{+0.24}	0.97 ± 0.05	1.01	0.98 ± 0.05
7.82 _{-0.40} ^{+0.24}	1.09 ± 0.05	1.02	1.11 ± 0.05
7.88 _{-0.14} ^{+0.10}	1.05 ± 0.05	1.02	1.07 ± 0.05
8.49 _{-0.13} ^{+0.09}	1.17 ± 0.05	1.03	1.21 ± 0.05
8.96 _{-0.32} ^{+0.19}	1.30 ± 0.05	1.07	1.39 ± 0.05
9.48 _{-0.20} ^{+0.16}	1.33 ± 0.05	1.10	1.46 ± 0.05
9.97 _{-0.19} ^{+0.14}	1.30 ± 0.05	1.15	1.49 ± 0.05
16.00 _{-0.3} ^{+0.3 a}	0.23 ± 0.02	1.38	0.32 ± 0.03

^a T(d,n)He⁴ neutrons.
^b Average of front and rear disks.
^c Includes fissions produced by D(d,n^p)D neutrons.

reference 7, are plotted in Fig. 2. In addition, there have been included some data by other investigators⁹ for the 13–15 Mev region. These latter, as may be seen, appear to be consistent with the present measurement at 16 Mev.

ACKNOWLEDGMENTS

The authors wish to express their appreciation to Mr. R. A. Nobles, who set up the gas target system and assisted with some of the irradiations; to Mr. C. J. Orth and to Mrs. J. B. Panowski, who carried out the Mo⁹⁹ analyses; to Mrs. P. Armijo, who assisted with the U²³⁷ analyses; to Mrs. R. C. Neal, who performed the beta counts; and to Dr. R. L. Henkel, who contributed valuable advice and assistance in the evaluation of the experimental data.

⁹ Graves, Conner, Ford, and Warren (to be published).